ARPN Journal of Engineering and Applied Sciences




# DETERMINATION OF RESERVOIR DRAINAGE AREA FOR CONSTANT-PRESSURE SYSTEMS BY CONVENTIONAL TRANSIENT PRESSURE ANALYSIS

Freddy Humberto Escobar[1], Mashhad Fahes[2], Rafael Gonzalez[1], Diego Mauricio Pinchao[1] and Yu Long Zhao[3]
[1]Universidad Surcolombiana/CENIGAA, Avenida Pastrana - Cra, Neiva, Huila, Colombia
[1]The University of Oklahoma, Mewbourne School of Petroleum and Geological Engineering, Boyd St. SEC Rm, Norman, Ok USA
[3]State Key Laboratory of Oil and Gas Reservoir, Geology and Exploitation, Southwest Petroleum University, Xindu Street, xindu district, Chendu, Sichuan, P. R. China
E-Mail: fescobar@usco.edu.co

**ABSTRACT**

The conventional straight-line method of transient pressure analysis implies drawing a straight line whose slope and intercept are used for parameter estimation, i.e., the slope and intercept of the semilog plot will lead to the estimation of permeability and mechanical skin factor respectively. For closed systems, the slope on a Cartesian plot of the late pseudosteady-state region allows estimation of the drainage area. For constant-boundary systems, the slope is zero, and as a result the drainage area would be estimated to have an infinite value. Because of this situation, a new way of using conventional analysis ought to be applied, and this constitutes the sole purpose of this work. By drawing a horizontal line at which the steady-state period takes place and observaing the time at which this regime starts, it is possible to find the drainage area. Contrary to closed systems, for constant-pressure boundary the reservoir geometry affects the starting time of steady-state period, consequently, separate solutions must be provided according to the well position and reservoir geometry. Although, one equation was formulated, six different constants are provided that have specific application depending upon well location and reservoir geometry. The proposed equation was verified with synthetic and field examples.

**Keywords:** pressure transient analysis, fracture conductivity, fracture half-length, *TDS* technique, elliptical flow, naturally fractured reservoirs.

## 1. INTRODUCTION

Jones (1957) introduced the reservoir limit tests from the analysis of long drawdown tests. He studied the pressure behavior once radial flow vanished and the closed pressure boundary was responsible for the pressure behavior. Under these circumstances, well pressure drop was directly proportional to testing time so reservoir area could be estimated from a Cartesian plot of pressure versus time. Earlougher *et al*. (1968), using the superposition principle, extended the unsteady-state solution for a cylindrical, constant pressure well in an infinite medium to almost any type of geometrical reservoir shape. The first solution for the estimation of the reservoir drainage area in closed reservoirs by buildup pressure transient analysis was introduced by Ramey and Cobb (1971) using the slope of a Cartesian plot during the late pseudosteady-state flow regime. Earlougher (1971) used the intercept of the pressure-versus-time Cartesian plot to estimate the shape factor previously introduced by Dietz (1965). More than two decades later, Tiab (1994) introduced a more practical and easy-to-use solution from the pressure derivative versus time log-log plot which uses the point of intersection between the late-time pseudosteady-state periods with the extrapolation of the horizontal radial flow regime straight line found as part of the *TDS* technique, Tiab (1993). This solution works perfectly in circular, square or rectangular closed systems, but it fails to provide accurate results for constant-pressure systems having a rectangular or elongated geometry, therefore, its application as currently implemented leads to severe mistakes in the estimation of the reservoir drainage area. Another solution presented by Chacón, Djebrouni and Tiab (2004) uses any arbitrary time and pressure derivative point reading during the late-time pseudosteady-state period to easily and exactly provide an estimation of reservoir drainage area in closed systems. A great advantage of this solution is the fact that it does not involve reservoir permeability in the calculations and can be used even when the radial flow data is highly noisy. However, care should be taken in designing and running the test long enough so the late-time pseudostate-steady state period is well developed. For noisy data, it is recommended to extrapolate the straight line on late pseudosteady-state flow regime so it can be read at the time of 1 hr.

However, all the above estimations of the drainage area apply indistinctively only to closed boundary systems. For the constant-pressure boundary case, the situation is different since the behavior changes markedly. This is especially so in elongated systems such as channels or wells between parallel faults, which of course are subjected to a constant-pressure lateral

VOL. 10, NO. 12, JULY 2015 ISSN 1819-6608
ARPN Journal of Engineering and Applied Sciences



boundary. For such cases, Escobar, Tiab and Hernandez (2004) extended the *TDS* Technique, Tiab (1993).

The aim of the present work is to complement Escobar *et al*. (2004)'s work for finding the drainage area in constant-pressure boundary reservoirs under conventional analysis. For this, the dimensional time based on area at which steady-state develops was used for a variety of well positions along an elongated reservoir having one or both parallel boundaries at constant pressure. It was also found that for circular and square geometrical shape, the dimensionless time based upon area was practically the same; consequently, the same area equation applies to both mentioned systems. The proposed solution was satisfactorily verified with synthetic and field cases and compared to the previous work of Escobar *et al*. (2004).

## 2. MATHEMATICAL FORMULATION

### 2.1. Dimensionless quantities

The dimensionless quantities are defined below as:

$$t_{DA} = \frac{0.0002637kt}{\phi \mu c_t A} \tag{1}$$

$$t_D = \frac{0.0002637kt}{\phi \mu c_t r_w^{\ 2}} \tag{2}$$

$$P_D = \frac{kh\Delta P}{141.2q\mu B} \tag{3}$$

$$t_D * P_D' = \frac{kh(t*\Delta P')}{141.2q\mu B} \tag{4}$$

The dimensionless time, Equation (1), at which a system responds is the same no matter the reservoir size. This implies that it is necessary to establish the dimensionless time response at which each well-reservoir configuration system reacts. This dimensionless time is referred to here as $(t_{DA})_{sss}$, the dimensionless time based on area at which the steady-state period starts.

### 2.2. Reservoir-well configurations

Several simulation runs were performed using the information of the second column in Table-1.

### 2.2.1. Centered well inside either a square or circular reservoir shape

Figure-1 shows the log-log pressure versus time behavior for a well centered inside either a square- or circular-shaped reservoir. As seen there, it is very difficult to discriminate the time at which the steady state starts. Therefore, more simulations were run for other square reservoir areas as reported in Figure-2. It is observed in both plots that $(t_{DA})_{sss} \approx 0.2365$. Then, substituting this value in Equation (1) and solving for the area, it yields:

$$A = \frac{kt_{sss}}{896.9\phi \mu c_t} \tag{5}$$

### 2.2.2. Well centered in rectangular systems

#### 2.2.2.1. One constant-pressure boundary

**Table-1.** Input data for examples and simulations.

| | | Examples | |
|---|---|---|---|
| **Parameter** | **Simulation runs** | **1, 2** | **Field** |
| $P_i$, psi | 5000 | 2500 | |
| $k$, md | 100 | 100 | 252.1 |
| $r_w$, ft | 0.3 | 0.3 | 0.3541 |
| $h$, ft | 30 | 100 | 40 |
| $\phi$, % | 10 | 10 | 20 |
| $B$, rb/STB | 1.25 | 1.25 | 1.04 |
| $\mu$, cp | 1 | 5 | 5 |
| $c_t$, 1/psi | $3\times10^{-6}$ | $1\times10^{-5}$ | $7.6\times10^{-6}$ |
| $q$, BPD | 300 | 500 | 150 |
| $Y_E$, ft | Several | 800 | |
| $X_E$, ft | Several | 5000 | |
| $b_x$, ft | Several | 1000 | |

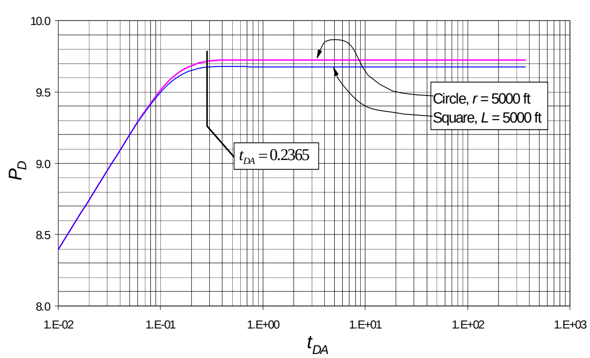


**Figure-1.** Comparison of the starting time of steady state for circular and square reservoir shapes (centered well).

VOL. 10, NO. 12, JULY 2015 ISSN 1819-6608
ARPN Journal of Engineering and Applied Sciences

www.arpnjournals.com

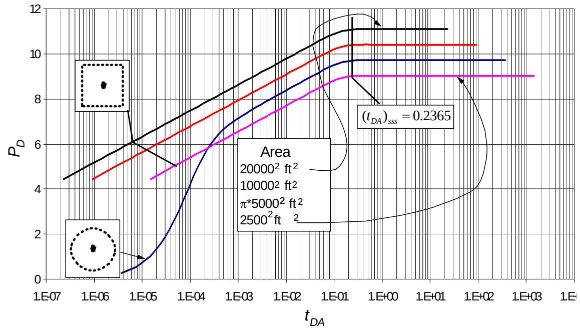


**Figure-2.** Well at the center of a circular and squares geometrical shapes. Constant-pressure boundary.

Escobar, Hernandez and Hernandez (2007) and Escobar *et al*. (2010) presented the dimensionless pressure derivative governing equation for these systems.

$$t_D * P_D' = \frac{32W_D^2}{19\pi}\left(\frac{X_E}{Y_E}\right)^3 t_D^{-1} \tag{6}$$

This considers that a negative unit-slope line goes tangential to the steady-state flow period. As a result, integrating Equation (6) to obtain the dimensionless pressure behavior is meaningless.

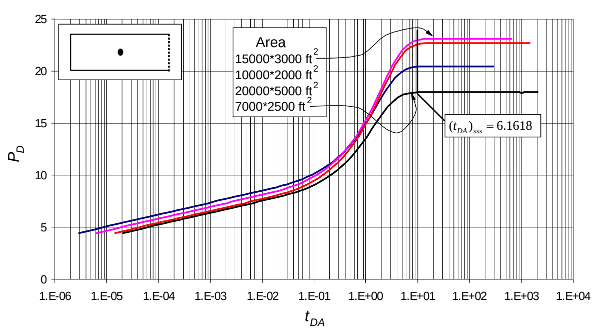


**Figure-3.** Well at the center of a rectangular-shaped reservoir. One lateral boundary at constant pressure.

From Figure-3, it is empirically observed that the dimensionless time at which the steady-state flow period starts is 6.1618. This indicates that its replacement into Equation (1) allows obtaining:

$$A = \frac{kt_{sss}}{23366.7\phi\mu c_t} \tag{7}$$

**2.2.2.2. Both constant-pressure boundaries**

As in the former case, the pressure derivative governing equation given by Escobar *et al*. (2004, 2007) for this specific well-reservoir configuration is given by:

$$t_D * P_D' = \frac{W_D^2}{5\pi}\left(\frac{X_E}{Y_E}\right)^3 t_D^{-1} \tag{8}$$

The integration of Equation (8) does not lead to a meaningful expression, and so, from observations of Figure-4, $(t_{DA})_{sss} \approx 2.647$, which leads to find:

$$A = \frac{kt_{sss}}{10037.93\phi\mu c_t} \tag{9}$$

**2.2.3. Well off-centered**

**2.2.3.1. Far constant-pressure boundary and closed near lateral boundary**

Escobar *et al*. (2004, 2007) provided the governing pressure derivative equation for this flow behavior:

$$t_D * P_D' = \left(\frac{X_E}{Y_E}\right)^3 \frac{W_D^2}{t_D} \tag{10}$$

Figure-5 allows observing the starting dimensionless time of the steady-state flow period, which is about 11. This is replaced in Equation (1) to obtain:

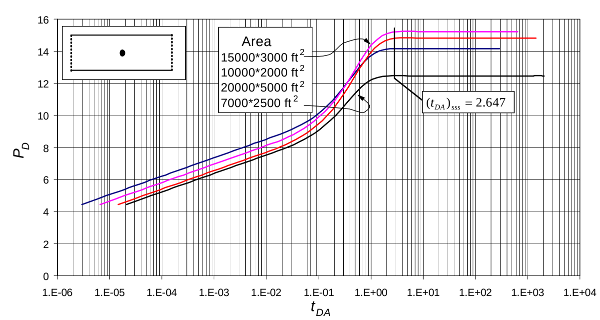


**Figure-4.** Well at the center of a rectangular-shaped reservoir. Both lateral boundaries at constant pressure.

VOL. 10, NO. 12, JULY 2015 ISSN 1819-6608
ARPN Journal of Engineering and Applied Sciences



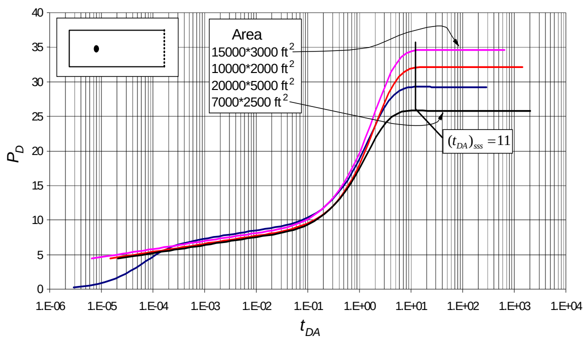


**Figure-5.** Well off-centered inside a rectangular-shaped reservoir. Far lateral boundary at constant pressure.

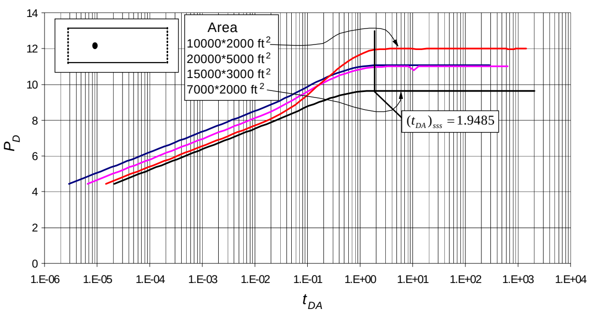


**Figure-6.** Well off-centered inside a rectangular-shaped reservoir. Both lateral boundary at constant pressure.

$$A = \frac{kt_{sss}}{41414\phi\mu c_t} \tag{11}$$

**2.2.3.2. Both constant-pressure boundaries**

This type of system allows the development of the parabolic flow, Escobar *et al*. (2005), which is also recognized as linear stabilization. Again, Escobar *et al*. (2004, 2007) provided the dimensionless pressure derivative governing equation;

$$t_D * P_D' = \left(\frac{W_D^2}{\pi^2}\right)\left(X_D^{1.5}\right)\left(\frac{X_E}{Y_E}\right)^3 \frac{1}{t_D} \tag{12}$$

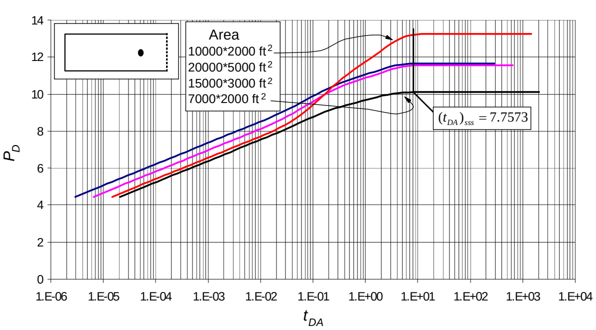


**Figure-7.** Well off-centered inside a rectangular-shaped reservoir. Near boundary is at constant pressure and far boundary is closed.

**Table-2.** Summary of area equations for conventional analysis.

| Constant, Ξ | Equation | Reservoir geometry |
|---|---|---|
| 869.9 | $A = \frac{kt}{\Xi\phi\mu c_t}$ | |
| 23366.7 | | |
| 10037.93 | | |
| 41414 | | |
| 7389.1 | | |
| 29417.2 | | |

**Table-3.** Summary of area equations for *TDS* technique, after Escobar *et al.* (2010).

| Constant, Ξ | Equation | Reservoir geometries |
|---|---|---|
| | $A = \frac{kt_{rpssi}}{283.66\phi\mu c_t}$ | |
| 4066 | $A = \sqrt[3]{\frac{kt_{ssri}Y_E^4}{\Xi\phi\mu c_t}}$ | |
| 482.84 | | |
| 7584.2 | | |
| 2173.52 | $A = \left(\frac{kt_{ss1ri,ss2ri}}{\Xi\phi\mu c_t}\right)^{2/3}\frac{Y_E^{5/3}}{b_x}$ | |
| 6828.34 | | |
| 41.82 | $X_E = \frac{1}{\Xi}\left(\frac{kt_x}{\phi\mu c_t}\right)^{0.5}$ | |
| 20.91 | | |

From Figure-6, it is seen that the stabilization or starting dimensionless time is 1.9485 which substituted in Equation (1) leads to obtain:

$$A = \frac{kt_{sss}}{7389.1\phi\mu c_t} \tag{13}$$

**2.2.3.3. Near boundary at constant pressure and closed far boundary**

ARPN Journal of Engineering and Applied Sciences



In this case, parabolic flow or linear stabilization is also developed. The governing dimensionless pressure derivative equation proposed by Escobar *et al*. (2004, 2007) is:

$$t_D * P_D' = \left(\frac{W_D^2}{\pi}\right)\left(X_D^{1.5}\right)\left(\frac{X_E}{Y_E}\right)^3 t_D^{-1} \quad (14)$$

The starting time of the steady-state flow period is about 7.7573 according to Figure-7 which allows finding:

$$A = \frac{kt_{sss}}{29417.2\phi\mu c_t} \quad (15)$$

Table-2 summarizes the developed equations and Table-3 summarizes the Equations obtained by Tiab *et al*. (2010) for the *TDS* technique.

## 3. METHODOLOGIA OF INTERPRETATION

For the estimation of the drainage area in constant-pressure boundary systems, it is required:

a) To build either a log-log of pressure/pressure drop versus time or a Cartesian plot of pressure/pressure drop versus time. Although, it is recommended to use a P-vs-t plot, then, draw a straight line (it should be horizontal) along the steady-state flow period. This is recognized because either pressure or pressure drop remains constant.

b) Then, identify the onset of the steady-state flow regime. In other words, read the time value at which the pressure or pressure drop starts being constant.

c) Identify the geometrical system dealt with for the application of one of the equations summarized in Table-2.

d) Estimate the drainage area.

## 4. EXAMPLES

For comparison purposes, three of the exercises worked by Escobar *et al.* (2010) will be used here.

### 4.1. Example 1

A pressure test was run using the third column in Table-1 as input data. Pressure versus time data are given in the Cartesian plot reported in Figure-8.

**Solution.** A starting time of the steady state, $t_{sss} \approx$ 6000 hr is read from Figure-8. We know from Escobar et al (2010) that this configuration corresponds to a well near a constant-pressure boundary and having closed the other one. Then dual linear and parabolic flows are developed. Since the reservoir geometry is known then Equation (15) applies:

$$A = \frac{100\text{ md}(8300\text{ hr})(800\text{ ft})^4}{29417.2(0.1)(5\text{ cp})(1\times10^{-5}\text{ psi}^{-1})} = 4079246\text{ ft}^2$$

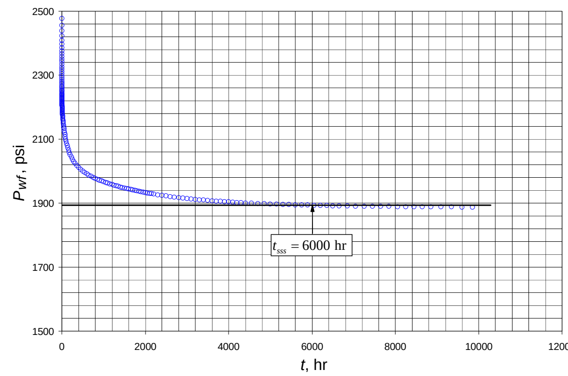


**Figure-8.** Cartesian plot of pressure-versus-time data for example 1.

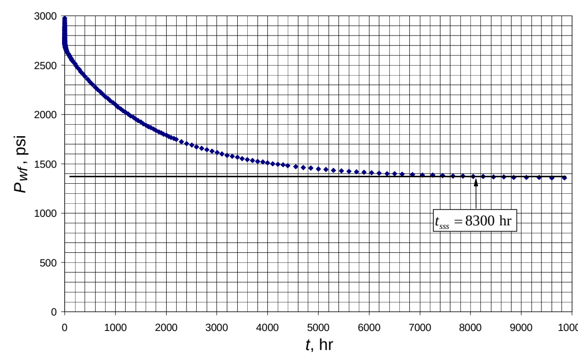


**Figure-9.** Cartesian plot of pressure-versus-time data for example 2.

### 4.2. Example 2

Figure-9 reports a Cartesian plot of pressure versus time data for a well near a closed boundary and far from the constant-pressure boundary which implies the development of both dual linear or single (hemilinear) flow regimes.

**Solution.** Once the horizontal line is drawn through the late data in Figure-9 a value of $t_{sss} \approx$ 8300 hr is read and used in Equation (11):

$$A = \frac{100\text{ md}(8300\text{ hr})(800\text{ ft})^4}{41414(0.1)(5\text{cp})(1\times10^{-5}\text{ psi}^{-1})} = 4008306\text{ ft}^2$$

### 4.3. Field example

VOL. 10, NO. 12, JULY 2015 ISSN 1819-6608
ARPN Journal of Engineering and Applied Sciences

www.arpnjournals.com

This example also reported by Escobar *et al*. (2010) has relevant information in the fourth column of Table-1. Cartesian and pressure derivative plots are reported in Figures-10 and 11, respectively.

**Solution.** This test is noisy and the reservoir looks to have a slight rectangular shape since linear flow regimes attempt to develop. Escobar *et al*. (2010) reported that a simulation was performed but the matching was not appropriate. The simulation provided a drainage area of 242,696 ft$^2$ for a circular model with a radius of 278.1 ft. It is known that the system is not fully circular, and so, the reference value is not trustable. Once the horizontal line is drawn through the late data in Figure-10 a value of $t_{sss} \approx 9$ hr is read and used in Equation (5):

$$A=\frac{252.1\,\text{md}(9\,\text{hr})}{896.9(0.2)(5\text{ cp})(7.6\times10^{-6}\text{ psi}^{-1})}=343696\text{ ft}^2$$

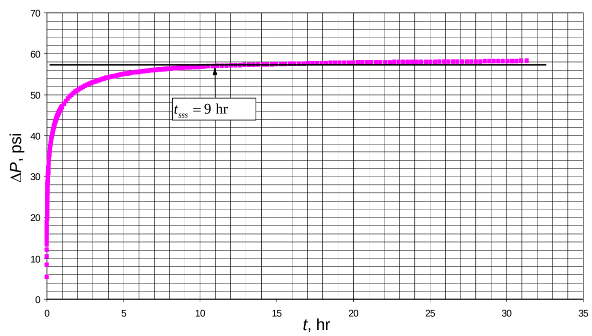


**Figure-10.** Cartesian plot of pressure drop versus time for field example.

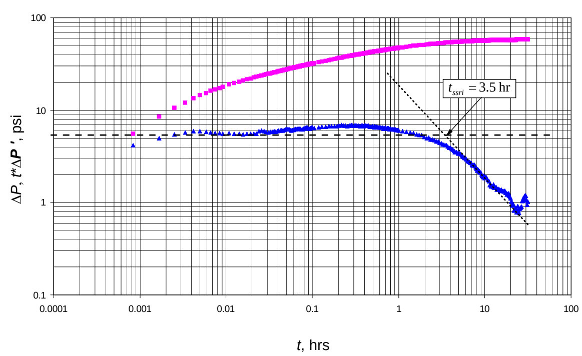


**Figure-11.** Pressure and pressure derivative versus time log-log plot for field example, after Escobar *et al*. (2010).

**Table-4.** A summary of results and a comparison with the *TDS* technique as reported by Escobar *et al.* (2010). The results are satisfactory and agree very well with the *TDS* technique.

| Example | Source | A, ft$^2$ | Absolute error, % |
|---|---|---|---|
| | Actual | 400000 | |
| 1 | *TDS* | 4450600 | 11.3 |
| | This work | 4079246 | 1.98 |
| 2 | Actual | 4000000 | |
| | *TDS* | 3878150 | 3.05 |
| | This work | 4008306 | 0.2 |
| Field | Actual | 242696 | |
| | *TDS* | 335164 | 41.4 |
| | This work | 343696 | 38.1 |

**5. CONCLUSIONS**

Conventional analysis was implemented for circular, square and rectangular system subject to constant-pressure boundaries. The developed equations successfully applied to synthetic and field examples are used by drawing a line throughout the point during steady-state period so the onset or initiation of the steady-state is used for finding the drainage area.

**ACKNOWLEDGEMENTS**

The authors thank Universidad Surcolombiana, the University of Oklahoma and the National Science Fund for Distinguished Young Scholars of China (Grant No. 51125019) and the National Program on Key Basic Research Project (973 Program, Grant No. 2011CB201005), and the Natural Science Foundation of China (Grant No.51374181).

**Nomenclature**

| | |
|---|---|
| $A$ | Area, ft$^2$ |
| $B$ | Oil formation factor, bbl/STB |
| $b_x$ | Distance from the to the near lateral boundary, ft |
| $C_A$ | Shape factor |
| $c_t$ | Compressibility, 1/psi |
| $h$ | Formation thickness, ft |
| $k$ | Permeability, md |
| $P$ | Pressure, psi |
| $P_D$ | Dimensionless pressure |
| $P_i$ | Initial reservoir pressure, psia |
| $P_{wf}$ | Well flowing pressure, psi |
| $q$ | Flow rate, bbl/D |
| $r_e$ | Drainage radius, ft |
| $r_w$ | Well radius, ft |
| $t$ | Time, hr |

ARPN Journal of Engineering and Applied Sciences



| | |
|---|---|
| $t_D$ | Dimensionless time based on well radius |
| $t_{DA}$ | Dimensionless time based on reservoir drainage area |
| $t_D*P_D$' | Dimensionless pressure derivative |
| $X_E$ | Reservoir length, ft |
| $X_D$ | Dimensionless reservoir length |
| $Y_E$ | Reservoir width, ft |
| $W_D$ | Dimensionless reservoir width |

**Greek**

| | |
|---|---|
| $\Delta$ | Change, drop |
| $\Delta t$ | Flow time, hr |
| $\phi$ | Porosity, fraction |
| $\mu$ | Viscosity, cp |

**Suffices**

| | |
|---|---|
| *D* | Dimensionless |
| *i* | Intersection or initial conditions |
| *L* | Linear |
| *PB* | Parabolic |
| *pss* | Pseudosteady |
| *SS* | Steady |
| *DLPSSi* | Intersection of pseudosteady-state line with dual- linear line |
| *ss*1*ri* | Intersection between the radial line and the -1-slope line |
| *ss*2*ri* | Intersection of radial line with -1-slope line (*SS*2) |
| *ssri* | Intersection of radial line with -1-slope line (*SS*2) |
| *sss* | Start of steady state |
| *r* | radial flow |
| *w* | Well |
| *x* | Maximum point (peak) after dual linear flow is vanished and steady state begins |

## REFERENCES

Chacon A., Djebrouni A. and Tiab D. 2004, January 1. Determining the Average Reservoir Pressure from Vertical and Horizontal Well Test Analysis Using the Tiab's Direct Synthesis Technique. Society of Petroleum Engineers. doi:10.2118/88619-MS.

Dietz D. N. 1965, August 1. Determination of Average Reservoir Pressure From Build-Up Surveys. Society of Petroleum Engineers. doi:10.2118/1156-PA.

Earlougher R. C., Ramey H. J., Miller F. G. and Mueller T. D. 1968, February 1. Pressure Distributions in Rectangular Reservoirs. Society of Petroleum Engineers. doi:10.2118/1956-PA.

Earlougher R. C. 1971, October 1. Estimating Drainage Shapes from Reservoir Limit Tests. Society of Petroleum Engineers. doi:10.2118/3357-PA.

Escobar F.H., Hernandez Y.A. and Tiab D. 2010. Determination of reservoir drainage area for constant-pressure systems using well test data. CT and F - Ciencia, Tecnología y Futuro. 4(1): 51-72.

Escobar F.H., Hernández Y.A. and Hernández C.M. 2007. Pressure Transient Analysis for Long Homogeneous Reservoirs using TDS Technique. Journal of Petroleum Science and Engineering. ISSN 0920-4105. 58(1-2): 68-82.

Escobar F.H., Muñoz O.F., Sepulveda J.A. and Montealegre M. 2005. New Finding on Pressure Response In Long, Narrow Reservoirs. CT and F - Ciencia, Tecnología y Futuro. 2(6): 151-160. ISSN 0122-5383.

Jones P. 1957, January 1). Drawdown Exploration Reservoir Limit, Well and Formation Evaluation. Society of Petroleum Engineers. doi:10.2118/824-G.

Tiab D. 1993. Analysis of Pressure and Pressure Derivative without Type-Curve Matching: 1- Skin and Wellbore Storage. Journal of Petroleum Science and Engineering. 12: 171-181.

Tiab D. 1994. Analysis of Pressure and Pressure Derivative without Type Curve Matching: Vertically Fractured Wells in Closed Systems. Journal of Petroleum Science and Engineering. 11: 323-333.

Ramey H.R., Jr. and cobb W.M. 1971. A general Buildup Theory for a Well in a Closed Drainage Area. JPT Dec. pp. 1493-1505.